



Repositorio Institucional de la Universidad Autónoma de Madrid

<https://repositorio.uam.es>

Esta es la **versión de autor** del artículo publicado en:

This is an **author produced version** of a paper published in:

Journal of the American Chemical Society 135.6 (2013): 2052 -2055

DOI: <http://dx.doi.org/10.1021/ja3100116>

Copyright: © 2013 American Chemical Society

El acceso a la versión del editor puede requerir la suscripción del recurso

Access to the published version may require subscription

A Molecular Platinum Cluster Junction: A Single-Molecule Switch

Linda A. Zotti,^{*,†} Edmund Leary,^{†,‡} Maria Soriano,^{†,¶} Juan Carlos Cuevas,[§] and Juan Jose Palacios[†]
Departamento de Física de la Materia Condensada, Universidad Autónoma de Madrid, 28049 Madrid, Spain, Inst Madrilenio Estudios Avanzados Nanociencia IMDEA, E-28049 Madrid, Spain, Departamento de Física Aplicada, Universidad de Alicante, 03690 Alicante, Spain, and Departamento de Física Teórica de la Materia Condensada, Universidad Autónoma de Madrid, E-28049 Madrid, Spain

Received February 27, 2013; E-mail: linda.zotti@uam.es

Abstract: We present a theoretical study of the electronic transport through single-molecule junctions incorporating a Pt₆ metal cluster bound within an organic framework. We show that the insertion of this molecule between a pair of electrodes leads to a fully atomically-engineered nano-metallic device with high conductance at the Fermi level and two sequential high on/off switching states. The origin of this property can be traced back to the existence of a HOMO which consists of two degenerate and asymmetric orbitals, lying close in energy to the Fermi level of the metallic leads. Their degeneracy is broken when the molecule is contacted to the leads, giving rise to two resonances which become pinned close to the Fermi level and display destructive interference.

Molecular metal clusters have recently started being explored in breakjunction type single-molecule-conductance experiments,^{1–3} whilst previous studies have also investigated clusters in the STM-STS configuration which maintains a tunnel gap between the tip and the molecule.^{4,5} Clusters have fewer metal atoms than metal nanoparticles but a more precisely defined composition and structure and as such they are better suited for comparative studies between theory and experiments. Bare metal clusters have been successfully deposited and studied on various surfaces.^{6,7} Such clusters however require very clean conditions for study due to their high reactivity. In order to overcome this fact, and study molecules under the normal ambient conditions of the breakjunction experiment, the metal atoms must be encapsulated in a ligand sphere to avoid unwanted chemical reactions with the atmosphere. Ligand stabilized metal clusters (in particular those incorporated in an organic framework) have therefore been suggested as components of data storage devices where they would act as nano-capacitors due to their redox properties.⁸ Transport measurements on individual molecular metal clusters are, however, still rare. Metal atoms have been successfully incorporated into organic frameworks as metal complexes for single-molecule experiments, as well as chains of atoms.^{9–12} Regarding metal clusters, the Mn₁₂ structure has been investigated as the functional core in single molecule magnets¹ and theoretical studies about its transport properties have been carried out.^{13,14} However, despite the vast range of molecular clusters known, only a few have been analyzed in this context. This is especially true regarding the theory of the electronic transport.^{15,16}

In ref.,² single-molecule experiments on [Pt₆(μ-P^tBu₂)₄(CO)₄(S(CH₂)₄SH)₂]₃ (from now on (SC₄S)₂Pt₆) were carried out using the STM based I(s) technique.^{17,18} The structure of this Pt cluster makes it ideal for these kind of measure-

ments as the ligands which act as binding groups (the alkanethiol chains) are oriented trans to each other, producing a linear wire. Without these chains, it would be difficult to determine a precise point of attachment between the molecule and the electrodes. The presence of these groups not only provides robust thiol anchors, but also increases the total length of the molecule in one defined direction, allowing measured break-off distances to assess accurately the orientation of the molecule in the junction (the need of incorporating the metal cluster in a wire has also been suggested in a theoretical study of the electronic transport through a Mn₁₂ cluster¹⁴). In the experimental study, it was suggested that the presence of the platinum cluster increases the conductance compared to an alkane chain of equivalent length due to there being Pt states in close proximity to the Fermi level. These were claimed to create an indentation in the potential barrier, giving a molecular analog of an inorganic double tunneling barrier, with the Pt₆ unit acting as a well and the alkane chains acting as barriers so to decouple the central unit from the leads. This was, however, a speculative argument which was never fully proven, and neither was the nature of these states identified. Finding out whether this assertion could be true is important because the molecular double tunneling barrier configuration could be the basis for creating molecular switches,¹⁹ analogous of conventional electronic components. This is ultimately one of the main aims of molecular electronics.²⁰ In this study presented here, we carried out first principle calculations to find out if we could corroborate the assumptions made in the experimental work. We will show that the HOMO of (SC₄S)₂Pt₆ consists of two degenerate levels which get pinned to the Fermi level when the molecule is placed between two gold electrodes. However, these two levels do not originate simply from the Pt₆ unit, but contain states localized on the ligands also. Moreover, interesting interference features appear in the transmission curve at the Fermi level.

We optimized all geometries with Turbomole 6.1,²¹ using the BP86 functional²² and the def-SVP basis set.²³ We built the molecular junctions by placing the molecules (previously relaxed in the gas phase) between two 20 gold atom clusters and then relaxed the molecule and the 4(3) innermost gold atoms on each side in a top (hollow) geometry. The subsequent transport calculations were carried out with ANT,²⁴ which is built as an interface to Gaussian.²⁵ This code computes the electronic transmission using nonequilibrium Green's function techniques in the spirit of the Landauer formalism, employing parametrized tight-binding Bethe lattices in the electrode description.²⁶ For these calculations, we used the PBE functional,²⁷ a lan12DZ basis set for Pt atoms and the four innermost Au atoms on each side,²⁸ while we used a CRENBS basis set²⁹ for all the other Au atoms. A 6-31++G basis set was chosen for C, S, P, O, and sto-3g for H.

We first studied the molecule in the gas phase. The optimized geometry is shown in 1. It consists of a Pt₆ cluster sandwiched between two butanedithiol (four carbon atoms) chains. The cen-

[†]Universidad Autónoma de Madrid

[‡]Inst Madrilenio Estudios Avanzados Nanociencia IMDEA, E-28049 Madrid, Spain

[¶]Universidad de Alicante

[§]Universidad Autónoma de Madrid

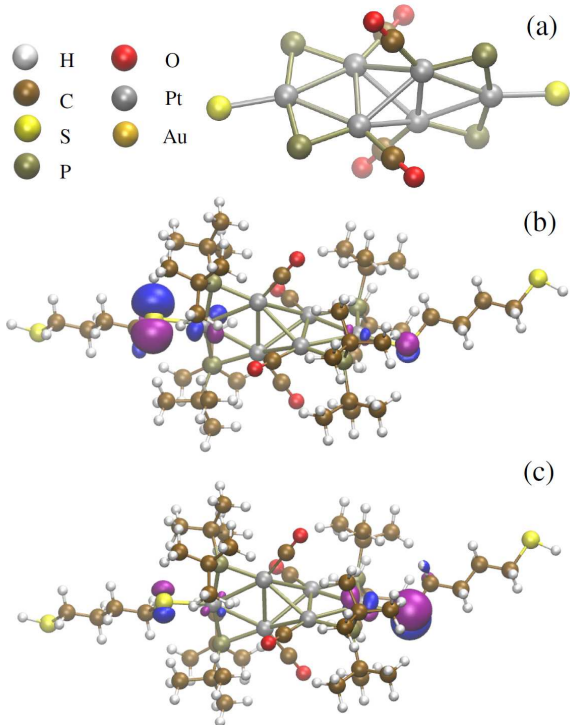


Figure 1. Central moiety of $(SC_4S)_2Pt_6$ (a) and optimized geometry of the whole molecule with the two degenerate HOMO orbitals (b-c).

tral cluster consists in turn of two orthogonal Pt_3 triangles, confirmed by crystallographic structural determination on the carbonyl substituted compound.³⁰ Each Pt_3 triangle contains two bridging phosphine groups and the remaining sides are joined together to form a Pt tetrahedral core. The tetrahedral core also contains four CO ligands. The molecule is slightly bent, with the angle between the alkyl chains less than 180° . In the second and third panel of 1 we show the HOMO. It consists of two doubly occupied levels which are degenerate and the corresponding orbitals of which are related to each other by a 4-fold improper rotation. It is mainly localized on the two innermost S atoms and on the two neighboring Pt atoms. Notice that these frontier orbitals are different from the HOMO shown in ref³⁰ due to the presence of the butanedithiol ligands. We also studied a $C_{18}H_{36}$ alkyl chain terminated with S atoms (from now on C_{18}), as it was claimed² to have the same length as $(SC_4S)_2Pt_6$ but a much lower conductance. Such a comparison would help us decide whether the presence of the Pt cluster provides a significant change in the conductance with respect to the alkyl chain alone. We first checked that the length of this chain provides a reasonable comparison to the cluster molecule. The length of C_{18} is 24.9 Å, which is halfway between the through space S to S distance (23.9 Å) and the length measured by adding the 3 components (2 chains + Pt core, 25.8 Å) in $(SC_4S)_2Pt_6$. In C_{18} , the HOMO is localized on the S atoms, while the HOMO-1 is delocalized throughout the whole chain²⁰.

After analyzing the molecules in the gas phase, we proceeded to study junctions containing $(SC_4S)_2Pt_6$ and C_{18} bound to the gold clusters in a top and a hollow geometry (2). 3 shows the transmission curves for all four cases. In the case of C_{18} , the energy alignment seems to be considerably affected by the binding geometry. In the hollow geometry, the HOMO-1 (which is delocalized throughout the whole chain and gives the main contribution to the transmission²⁰) is shifted down in energy compared to the top position (as has also been observed for other thiolated molecules³¹), yielding a

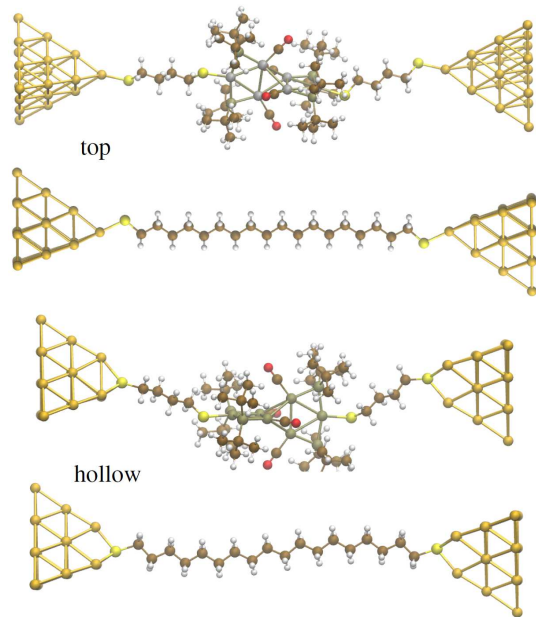


Figure 2. (Color online) Optimized geometries for $(SC_4S)_2Pt_6$ and C_{18} embedded between Au clusters.

difference in the conductance of one order of magnitude between the two geometries. Notice also the presence of the HOMO (localized on the S atoms) very close to the Fermi level, clearly visible as a bump in the transmission curve for the top geometry. In the case of $(SC_4S)_2Pt_6$, the alignment of the HOMO states does not show a particular dependence on the binding geometry as they are pinned at the Fermi level in both cases, but rather their splitting seems to be affected. The degeneracy of the HOMO states is broken in the junction as the symmetry has changed upon geometry relaxation. We stress that the two peaks close to the Fermi level do not arise simply from the Pt_6 unit as suggested in ref.,² but rather from orbitals which contain both S and Pt contribution, which however do not spread over all Pt atoms, as discussed above.

Fermi level pinning has been widely studied but its nature is still under discussion (see ref³² and references therein). It is also well known that molecular HOMO-LUMO gaps are usually underestimated in DFT and that this affects the conductance values in DFT-based transmission calculations. In order to gain insight into the level alignment in our calculations and to understand whether it is reliable, we evaluated the ionization potential (IP) and electron affinity (EA) in the gas phase for the two molecules, as $E(N) - E(N - 1)$ and $E(N + 1) - E(N)$, respectively, where N is the total electron number. These quantities (based on total-energy differences) are expected to be more reliable than the HOMO and LUMO assigned by the Kohn-Sham states (at -4.27 and -3.07 eV for $(SC_4S)_2Pt_6$ and at -5.3 and -0.08 eV for C_{18} , respectively). The calculated IP and EA in the gas phase were found to be at -5.66 and -1.70 eV for $(SC_4S)_2Pt_6$, and -7.4 and 0.45 eV for C_{18} , respectively. Molecular HOMO-LUMO gaps are expected to narrow when molecules approach metal electrodes due to the screening effect.³³ In the case of $(SC_4S)_2Pt_6$, since the IP is very close to the Au Fermi level (which is at -5.0 eV), it is plausible that contacting the molecule to the electrode raises the IP until such a point that it becomes pinned to the Fermi level. This is accompanied by a charge transfer from the molecule onto the metal, confirmed by 1.47 and 4.3 e positive charge found on the molecule in the top and hollow position, respectively. Notice that the transferred charge originates

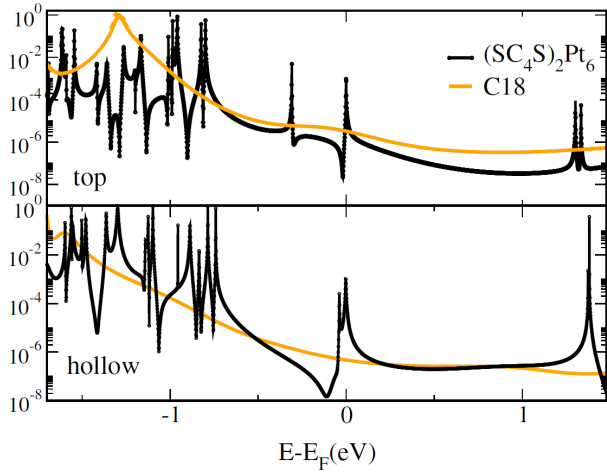


Figure 3. Transmission as a function of energy for all studied molecular junctions.

mostly from the S atoms directly connected to the leads. Based on the proximity of the IP to the gold Fermi level, we believe that the energy alignment of the HOMO states appearing in our transmission curves for $(\text{SC}_4\text{S})_2\text{Pt}_6$ is robust and unaffected by common DFT failures, providing a realistic picture of the experimental scenario. On the other hand, in the case of C_{18} , the IP calculated in the gas phase is at a much lower energy than the peak corresponding to the HOMO (localized on the S atoms) in the transmission curve for the Au- C_{18} -Au junction, especially for the top binding geometry. This suggests that it should align at lower energy; if so, the conductance values of C_{18} would be significantly lower than those which we computed.

A further significant result is the presence of interference resonances in the transmission curves, which are clearly visible in 3. The interest in interference effects in molecular junctions is steadily growing^{34–37} and this stems from the fact that they modify the thermoelectric properties of the junctions²⁰ and that the ensuing dips in the transmission curves could give rise to large on/off ratios in future molecule-based electronic devices.³⁶ Interference effects have recently been detected experimentally in molecular junctions.³⁸ In our case, they originate from the existence of two possible pathways (the two HOMO states). For the top position, we find a similar feature to that produced in ref.³⁹ Interferences yielding peaks at the Fermi level have already been predicted,^{40,41} however their occurrence from two degenerate levels pinned at the Fermi level, to the best of our knowledge, is rare. In order to shed light on the origin of these interference features, we built a simple model as depicted in 4, where we consider two levels both connected to the leads. They are related to the two HOMO levels of $(\text{SC}_4\text{S})_2\text{Pt}_6$, which are degenerate and orthogonal in the gas phase. However, when the molecule is placed between two electrodes, the symmetry and consequently the degeneracy is broken due to the geometrical readjustment of the molecule. Thus, in our model, we consider two states which are no longer eigenstates of the system and are coupled by a non-zero hopping matrix element t .

In this model, the Hamiltonian of the central (molecular) part takes the following form:

$$H_C = \begin{pmatrix} \varepsilon_0 & t_2 & t_1 & t_{14} \\ t_2 & \varepsilon_2 & t & t_1 \\ t_1 & t & \varepsilon_1 & t_2 \\ t_{14} & t_1 & t_2 & \varepsilon_0 \end{pmatrix}$$

where ε_1 and ε_2 are the energies of two degenerate molecular levels,

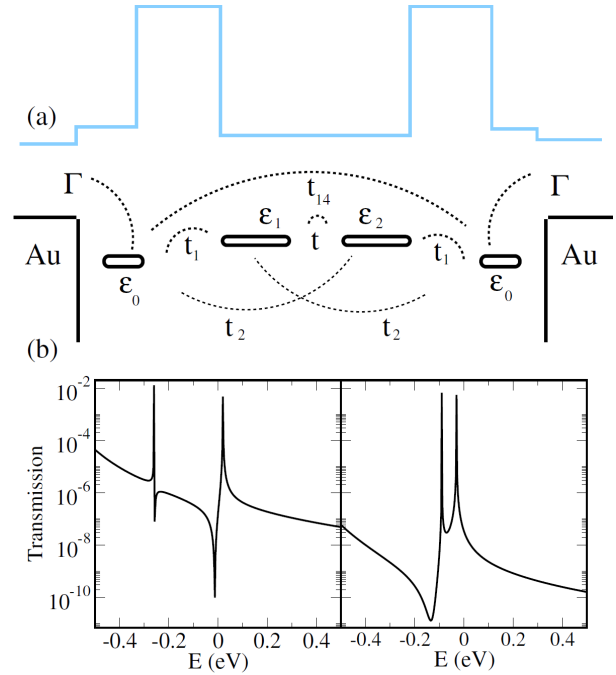


Figure 4. (a) Schematic representation (black) of the toy model describing the interference effects close to the Fermi energy and of the double tunnel barrier (blue). (b) The corresponding transmission as a function of energy for the case of the top position (left panel) with the following parameter values: $\Gamma = 0.05$ eV, $\varepsilon_0 = -0.7$ eV, $\varepsilon_1 = \varepsilon_2 = -0.12$ eV, $t_1 = 0.009$ eV, $t_2 = 0.005$ eV, $t = 0.14$ eV, $t_{14} = 0.003$ eV, and for the hollow geometry (right panel) with the parameter values: $\Gamma = 0.05$ eV, $\varepsilon_0 = -0.7$ eV, $\varepsilon_1 = \varepsilon_2 = -0.06$ eV, $t_1 = 0.005$ eV, $t_2 = 0.002$ eV, $t = 0.03$ eV, $t_{14} = 0.000145$ eV.

coupled to each other via t . ε_0 is the energy of the interface levels, coupled to ε_1 and ε_2 through t_1 and t_2 . Notice that t_1 must be bigger than t_2 , in order to account for the asymmetry of each orbital. The transmission is given by

$$T(E) = 4\Gamma_L\Gamma_R|G_{14}|^2 \quad (1)$$

where

$$G = [E - H_C - \Sigma]^{-1} \quad (2)$$

and $\Sigma = \Sigma_L + \Sigma_R$, being Σ_L and Σ_R the self energies for left and right lead, respectively. These two matrices have all terms equal to 0 but $\Sigma_{L11} = i\Gamma_L$ and $\Sigma_{R44} = i\Gamma_R$, being Γ_L and Γ_R the coupling to left and right lead, respectively. In our case, $\Gamma_L = \Gamma_R = \Gamma$ as we are considering symmetric junctions.

As an example, in the inset of 4 we show the transmission curve given by this model for a chosen set of parameters (listed in the caption) which can reproduce the shape of the DFT-calculated transmission curve for both hollow and top position. This proves that the nature of the features appearing in the transmission curves at the Fermi level is in the interference between the two levels of the central moiety and two levels localized at the interface between this central part and the leads. In the case of asymmetric junctions, such as top-hollow, the transmission curve is expected to resemble that corresponding to the top-top case (see the Supporting Information).

As mentioned above, the presence of a resonance immediately followed by an antiresonance increases the on/off ratio in gating experiments. One can simply view this by imagining that the Fermi level (located at 0 eV) is shifted to more negative values along the energy axis: by doing this, in the top geometry, for instance, the Fermi level will cross a first sharp peak (*on*) and, after a very small shift, a sharp dip (*off*). This sequence is then repeated by shift-

ing the Fermi level further so as to cross the second resonance-antiresonance couple. Indeed, we propose that the low bias conductance of this system should be measured experimentally as a function of the gate voltage, in order to test the breaking of the degeneracy.

Finally, we compare our results with the experiments. In ref.,² a conductance of $3 \times 10^{-5} G_0$ was measured for $(SC_4S)_2Pt_6$, while the conductance of C_{18} was extrapolated from the experimental attenuation (beta) value measured for a series of shorter compounds as $6 \times 10^{-10} G_0$. It was argued that the alkyl chains in $(SC_4S)_2Pt_6$ simply act as spacers as the frontier orbitals lie far from the Fermi level, while the frontier orbitals of the central unit create a barrier indentation and, consequently, raise the conductance by approximately 6 orders of magnitude compared to C_{18} . In our results, it is true that precisely at the very Fermi level the conductance of $(SC_4S)_2Pt_6$ is definitely higher than C_{18} ; however, at other energies immediately below or above it, the conductance is comparable or even lower, especially as a result of the destructive interference. This could potentially explain some non-linearities observed in some of the I-V curves recorded experimentally (see the Supporting Information of ref²). It is also worth adding that, due to the uncertainty about the precise length of the Pt molecule, exactly comparing the conductances of $(SC_4S)_2Pt_6$ and C_{18} is somehow ambiguous, since, in our equilibrium geometries, C_{18} is straight (with only slight defects) whereas the cluster molecule is bent, with the Pt_6 cluster slightly out of the Au-Au axis. In the experiments though, the Pt molecule is probably straightened, due to the pulling stress applied. Regardless these uncertainties, the overall picture supports the naive idea based on the experimental finding, confirming the presence of resonances at the Fermi level arising from the presence of the central additional moiety in the molecular cluster.

In conclusion, we have theoretically studied single molecule junctions incorporating a Pt_6 cluster, showing that it acts in an analogous fashion to a double tunneling barrier due to two (originally degenerate) states which align at the Fermi level. These states do not, however, stem from the Pt unit alone, but specifically from two apical Pt atoms and their neighboring S atoms. This gives rise to quantum interference effects due to multiple electronic pathways through the molecule. Due to the pinning, these effects should be easily detectable experimentally. Despite the seemingly apparent complexity of the structure, all the physical properties arise from these four atoms alone, highlighting the delicate relationship between molecular structure and electrical properties. We propose that further chemical synthesis combined with theoretical calculations should be performed in order to explore more combinations of metal clusters with organic moieties. This could provide an alternate design strategy for molecular devices other than through purely organic molecules due to the wealth of different structures possible via inorganic chemistry. Recent progress in implementing a gate in single-molecule based devices⁴²⁻⁴⁵ allows us to predict for the studied molecule, with its controlled binding to the electrodes and with its two levels aligned at the Fermi level, that it could be used in a three-terminal device in which only a small gate voltage would be enough to pass through two high/low sequential switching states.

Acknowledgement This research was supported by the Comunidad de Madrid through the project NANOBIOIMAGNET S2009/MAT1726, by the Generalitat Valenciana through the project PROMETEO2012/011 and by the Spanish MICINN under the Grant Nos. FIS2010-21883 and CONSOLIDER CSD2007-0010. EL was funded by the EU through the ELFOS Network (FP7-ICT2009-6). We thank the CCC of Universidad Autónoma de Madrid for computational resources.

References

- (1) Heersche, H. B.; de Groot, Z.; Folk, J. A.; van der Zant, H. S. J.; Romeike, C.; Wegewijs, M. R.; Zoppi, L.; Barreca, D.; Tondello, E.; Corni, A. *Phys. Rev. Lett.* **2006**, *96*, 206801.
- (2) Leary, E.; van Zalinge, H.; Higgins, S. J.; Nichols, R. J.; de Biani, F. F.; Leoni, P.; Marchetti, L.; Zanello, P. *Phys. Chem. Chem. Phys.* **2009**, *11*, 5198.
- (3) Boardman, B. M.; Widawsky, J. R.; Park, Y. S.; Schenck, C. L.; Venkataraman, L.; Steigerwald, M. L.; Nuckolls, C. *J. Am. Chem. Soc.* **2011**, *133*, 8455.
- (4) Soldatov, E. S.; Gubin, S. P.; Maximov, I. A.; Khomutov, G. B.; Kolesov, V. V.; Sergeev-Cherenkov, A. N.; Shorokhov, V. V.; Sulaimankulov, K. S.; Suyatin, D. B. *Microelectron. Engn.* **2003**, *69*, 536.
- (5) Gubin, S. P.; Gulayev, Y. V.; Khomutov, G. B.; Kislov, V. V.; Kolesov, V. V.; Soldatov, E. S.; Sulaimankulov, K. S.; Trifonov, A. S. *Nanotechnology* **2002**, *13*, 185.
- (6) Yasumatsu, H.; Hayakawa, T.; Kondow, T. *Chem. Phys. Lett.* **2010**, *487*, 279.
- (7) Isomura, N.; Wu, X.; Watanabe, Y. *Journ. Chem. Phys.* **2009**, *131*, 164707.
- (8) Femoni, C.; Iapalucci, M. C.; Kaswalder, F.; Longoni, G.; Zacchini, S. *Coordin. Chem. Rev.* **2006**, *250*, 1580.
- (9) Park, J.; Pasupathy, A. N.; Goldsmith, J. I.; Chang, C.; Yaish, Y.; Petta, J. R.; Rinkoski, M.; Sethna, J. P.; Abruña, H. D.; McEuen, P. L.; Ralph, D. C. *Nature* **2002**, *417*, 722.
- (10) Ruben, M.; Landa, A.; Lörtscher, E.; Riel, H.; Mayor, M.; Görls, H.; Weber, H. B.; Arnold, A.; Evers, F. *Small* **2008**, *4*, 2229.
- (11) Mayor, M.; von Hänisch, C.; Weber, H. B.; Reichert, J.; Beckmann, D. *Angew. Chem.* **2002**, *41*, 1183.
- (12) Georgiev, V. P.; McGrady, J. E. *J. Am. Chem. Soc.* **2011**, *133*, 12590.
- (13) Renani, F. R.; Kirczenow, G. *Phys. Rev. B* **2011**, *84*, 180408.
- (14) Barraza-Lopez, S.; Park, K.; García-Suárez, V.; Ferrer, J. *J. Appl. Phys.* **2009**, *105*, 07E309.
- (15) Gerasimov, Y. S.; Shorokhov, V. V.; Soldatov, E. S.; Snigirev, O. V. *Proc. of SPIE* **2010**, *7521*, 75210U-1.
- (16) Gerasimov, Y. S.; Shorokhov, V. V.; Maresov, A. G.; Soldatov, E. S.; Snigirev, O. V. *J. Commun. Technol. El.* **2011**, *56*, 1483.
- (17) Haiss, W.; van Zalinge, H.; Higgins, S. J.; Bethell, D.; Höbenreich, H.; Schiffrin, D. J.; Nichols, R. J. *J. Am. Chem. Soc.* **2003**, *125*, 15294.
- (18) Nichols, R. J.; Haiss, W.; Higgins, S. J.; Leary, E.; Martin, S.; Bethell, D. *Phys. Chem. Chem. Phys.* **2010**, *12*, 2801.
- (19) Leary, E.; Higgins, S. J.; van Zalinge, H.; Haiss, W.; Nichols, R. J. *Chem. Comm.* **2007**, *38*, 3939.
- (20) Cuevas, J. C.; Scheer, E. *Molecular electronics: An introduction to theory and experiment*; World Scientific, 2010.
- (21) Ahlrichs, R.; Bär, M.; Häser, M.; Horn, H.; Kölmel, C. *Chem. Phys. Lett.* **1989**, *162*, 165.
- (22) Perdew, J. P. *Phys. Rev. B* **1986**, *33*, 8822.
- (23) Schäfer, A.; Horn, H.; Ahlrichs, R. *J. Chem. Phys.* **1992**, *97*, 2571.
- (24) Palacios, J. J.; Jacob, D.; Perez-Jimenez, A. J.; Fabian, E. S.; Louis, E.; Verges, J. A. *ALACANT ab initio quantum transport package*, see URL: <http://alacant.dfa.ua.es>
- (25) Frish, M. J.; Trucks, G. W.; et al.; H. B. S. *GAUSSIAN 03, Revision B.01, Gaussian, Inc., Pittsburg 2003*.
- (26) Jacob, D.; Palacios, J. J. *Journ. Chem. Phys.* **2011**, *134*, 044118.
- (27) Perdew, J. P.; Burke, K.; Ernzerhof, M. *Phys. Rev. Lett.* **1997**, *78*, 1396.
- (28) Wadt, W. R.; Hay, P. J. *J. Chem. Phys.* **1985**, *82*, 284.
- (29) Ross, R. B.; Powers, J. M.; Atashroo, T.; Ermiler, W. C.; LaJohn, L. A.; Christiansen, P. A. *J. Chem. Phys.* **1990**, *93*, 6654.
- (30) de Biani, F. F.; Ienco, A.; Laschi, F.; Leoni, P.; Marchetti, F.; Marchetti, L.; Mealli, C.; Zanello, P. *J. Am. Chem. Soc.* **2005**, *127*, 3076.
- (31) Zotti, L. A.; Kirchner, T.; Cuevas, J. C.; Pauly, F.; Huhn, T.; Scheer, E.; Erbe, A. *Small* **2010**, *6*, 1529.
- (32) Bokdam, M.; Cakir, D.; Brocks, G. *Appl. Phys. Lett.* **2011**, *98*, 113303.
- (33) García-Lastra, J. M.; Rostgaard, C.; Rubio, A.; Thygesen, K. S. *Phys. Rev. B* **2009**, *80*, 245427.
- (34) Bergfield, J. P.; Solomon, G. C.; Stafford, C. A.; Ratner, M. A. *Nano Lett.* **2011**, *11*, 2759.
- (35) Markussen, T.; Stadler, R.; Thygesen, K. S. *Nano Lett.* **2010**, *10*, 4260.
- (36) Nozaki, D.; Sevincli, H.; Avdoshenko, S. M.; Gutierrez, R.; Cuniberti, G. *arXiv:1203.5269v1*
- (37) Kaliginedi, V.; Moreno-García, P.; Valkenier, H.; Hong, W.; García-Suárez, V. M.; Buiterr, P.; Otten, J. L. H.; Hummelen, J. C.; Lambert, C. J.; Wandlowski, T. *J. Am. Chem. Soc.* **2012**, *134*, 5262.
- (38) Guedon, C. M.; Valkenier, H.; Markussen, T.; Thygesen, K. S.; Hummelen, J. C.; van der Molen, S. J. *Nat. Nanotechnol.* **2012**, *7*, 305.
- (39) Satani, A. M.; Hedin, E. R.; Joe, Y. S. *Phys. Lett. A* **2006**, *349*, 45.
- (40) Finch, C. M.; García-Suárez, V. M.; Lambert, C. J. *Phys. Rev. B* **2009**, *79*, 033405.
- (41) Wei, Z.; T.Li.; Jennum, K.; Santella, M.; Bovet, N.; Hu, W.; Nielsen, M. B.; Bjørnholm, T.; Solomon, G. S.; Laursen, B. W.; Nørsgaard, K. *Langmuir* **2012**, *28*, 4016.
- (42) Park, H.; Park, J.; Lim, A. K. L.; Anderson, E. H.; Alivisatos, A. P.; McEuen, P. L. *Nature* **2000**, *407*, 57.
- (43) Zhang, J.; Kuznetsov, A. M.; Medvedev, I. G.; Chi, Q.; Albrecht, T.; Jensen, P. S.; Ulstrup, J. *Chem. Rev.* **2008**, *108*, 2737.
- (44) Leary, E.; Higgins, S. J.; van Zalinge, H.; Haiss, W.; Nichols, R. J.; Nygaard, S.; Jeppesen, J. O.; Ulstrup, J. *J. Am. Chem. Soc.* **2008**, *130*, 12204.
- (45) Meded, V.; Bagrets, A.; Fink, K.; Chandrasekar, R.; Ruben, M.; Evers, F.; Bernard-Mantel, A.; Seldenthuis, J. S.; Beukman, A.; van der Zant, H. S. J. *Phys. Rev. B* **2011**, *83*, 245415.